AGU PUBLICATIONS

Geophysical Research Letters

RESEARCH LETTER
10.1002/2017GL075419

Key Points:
- The effect of present-day mass redistribution on ocean bottom deformation is studied
- A global mean ocean bottom subsidence of 0.1 mm/yr was caused by surface mass redistribution over 1993–2014
- Mean ocean basin deformations are 1 mm/yr in the Arctic Ocean and up to 0.4 mm/yr elsewhere

Correspondence to:
T. Frederikse,
t.frederikse@tudelft.nl

Citation:
Frederikse, T., Riva, R. E. M., & King, M. A. (2017). Ocean bottom deformation due to present-day mass redistribution and its impact on sea level observations. *Geophysical Research Letters*, *44*, 12,306–12,314. https://doi.org/10.1002/2017GL075419

Received 23 AUG 2017
Accepted 13 NOV 2017
Accepted article online 17 NOV 2017
Published online 23 DEC 2017

Ocean Bottom Deformation Due To Present-Day Mass Redistribution and Its Impact on Sea Level Observations

Thomas Frederikse[1], **Riccardo E. M. Riva**[1], **and Matt A. King**[2]

[1]Department of Geoscience and Remote Sensing, Delft University of Technology, Delft, Netherlands, [2]Surveying and Spatial Sciences, School of Land and Food, University of Tasmania, Hobart, Tasmania, Australia

Abstract Present-day mass redistribution increases the total ocean mass and, on average, causes the ocean bottom to subside elastically. Therefore, barystatic sea level rise is larger than the resulting global mean geocentric sea level rise, observed by satellite altimetry and GPS-corrected tide gauges. We use realistic estimates of mass redistribution from ice mass loss and land water storage to quantify the resulting ocean bottom deformation and its effect on global and regional ocean volume change estimates. Over 1993–2014, the resulting globally averaged geocentric sea level change is 8% smaller than the barystatic contribution. Over the altimetry domain, the difference is about 5%, and due to this effect, barystatic sea level rise will be underestimated by more than 0.1 mm/yr over 1993–2014. Regional differences are often larger: up to 1 mm/yr over the Arctic Ocean and 0.4 mm/yr in the South Pacific. Ocean bottom deformation should be considered when regional sea level changes are observed in a geocentric reference frame.

1. Introduction

Next to steric and dynamic changes, redistribution of mass between land and ocean is one of the major components driving global and regional sea level change (Chambers et al., 2016; Stammer et al., 2013). The redistribution causes distinct regional sea level change patterns, known as sea level fingerprints, which are caused by gravitational effects, changes in the Earth rotation parameters, and by deformation of the solid Earth (Clark & Lingle, 1977; Milne & Mitrovica, 1998). A substantial part of the regional pattern is caused by vertical deformation of the solid Earth that affects both land and the ocean bottom (King et al., 2012; Riva et al., 2017). Due to changes in the land ice mass balance and land hydrology, the oceans have gained mass over the past decades (Chambers et al., 2016), which results in an increase of the total load on the ocean bottom. Under this increasing load, the ocean floor will subside due to elastic deformation. This subsidence will increase the ocean basin capacity, given a constant geocentric ocean surface. Note that this elastic deformation has to be considered in addition to the viscoelastic response to past ice ocean mass changes, known as Glacial Isostatic Adjustment (GIA), for which sea level reconstructions are routinely corrected (Tamisiea, 2011). Ray et al. (2013) shows that the ocean bottom deformation caused by changes in ocean dynamics, atmospheric pressure, and land water storage (LWS) results in a substantial effect on the seasonal cycle in sea level derived from altimetry. However, in that study, ice mass changes, which have been the main cause of the ocean mass increase over the last two decades (Chambers et al., 2016), were excluded. In this paper, we examine how elastic deformation due to present-day ice mass and LWS changes has affected the shape of the ocean bottom over the last two decades and whether this deformation does affect trends in regional and global sea level reconstructions from tide gauges and altimetry.

Sea level changes are generally expressed in two distinct reference frames: either relative to the local ocean floor (relative sea level change) or relative to the Earth's center of mass (geocentric or absolute sea level change). Global mean sea level (GMSL) changes due to mass redistribution are called barystatic changes. These barystatic changes are defined as the total volume change of the ocean, divided by the ocean surface area. With this definition, barystatic changes are equal to relative sea level changes, integrated over the whole ocean. However, because of the deformation of the ocean bottom due to the changing load, global mean geocentric sea level changes resulting from mass changes are not equal to the barystatic changes. Since the solid

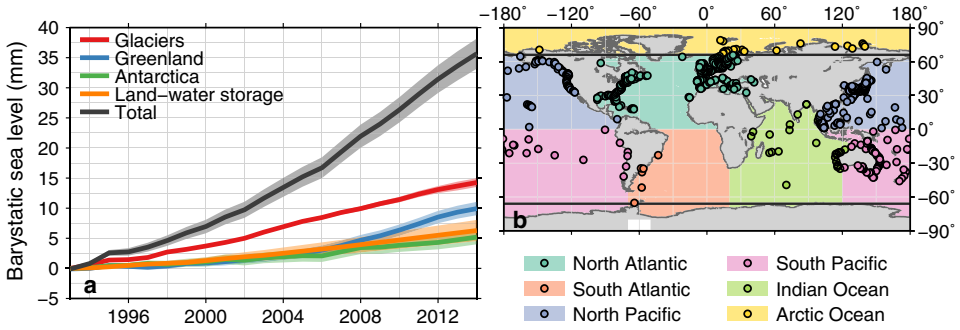

Figure 1. Modeled barystatic contributions and definition of the individual ocean basins. (a) Time series of the modeled barystatic sea level changes from each individual process and their sum. The shaded areas show the 1σ confidence interval. (b) Definition of each ocean basin. The dots show the tide gauge locations, and the color the basin to which each tide gauge is linked. The black lines show the upper and lower bounds of the altimetry domain.

Earth deformation is not uniform over the oceans, the regional or basin mean difference between relative and geocentric sea level change may deviate from the global mean difference.

The emergence of satellite altimetry has given a near-global overview of sea level changes (Nerem et al., 2010). However, because satellite altimetry observes sea level in a geocentric reference frame, global mean sea level estimates derived from altimetry will not observe the increase in ocean volume due to ocean bottom subsidence, and hence, they may underestimate GMSL rise. A correction associated with the elastic response to present-day mass redistribution is almost never applied (see Fenoglio-Marc et al., 2012; Kuo et al., 2008; Rietbroek et al., 2016 for exceptions), and altimetry-derived global mean sea level changes resulting from mass redistribution may thus differ from associated global ocean volume changes.

The launch of the Gravity Recovery And Climate Experiment (GRACE) satellite mission has allowed more detailed global and regional estimates of ocean mass changes and comparison with sea level changes (Chen et al., 2017; Kleinherenbrink et al., 2016; Leuliette & Willis, 2011). GRACE observations show ocean mass changes and hence show relative rather than geocentric sea level changes (Kuo et al., 2008; Ray et al., 2013), and the direct comparison between altimetry and GRACE will thus also introduce a bias when the effect of ocean bottom deformation is not corrected for.

On centennial timescales, sea level change estimates are mainly based on tide gauge data. As land-based instruments, they observe relative sea level. In the ideal case, when tide gauges sample the full ocean, they observe global ocean volume changes. In reality, tide gauges do not sample the whole ocean, and local vertical land motion (VLM) unrelated to large-scale sea level processes affects the observations, and therefore, correcting tide gauge records for VLM is desirable (Wöppelmann & Marcos, 2016). Traditionally, only the GIA component of VLM was modeled and corrected for. More recently, GPS, altimetry, and Doppler orbitography and radiopositioning integrated by satellite observations have been used to correct tide gauge records for VLM (Ray et al., 2010; Wöppelmann & Marcos, 2016). This correction brings tide gauges into a geocentric reference frame, and hence, the resulting global and regional sea level rise estimates may be biased due to ocean bottom deformation in the same way satellite-based estimates are.

In this paper, we study the difference in relative and geocentric sea level rise due to elastic deformation, given realistic estimates of present-day water mass redistribution to see to what extent the different observational techniques are affected. Based on recent estimates of mass changes related to ice, land water storage, and dam retention, we compute the resulting global mean and regional ocean bottom deformation. The impact on tide gauge-based sea level reconstructions is estimated by computing a synthetic "virtual station" sea level solution (Jevrejeva et al., 2006).

2. Methods and Data

The spatially varying response of the geoid, the solid Earth, and relative sea level to present-day mass exchange is computed by solving the elastic sea level equation (Clark & Lingle, 1977), which includes the Earth rotational feedback (Milne & Mitrovica, 1998). We solve the sea level equation using a pseudo-spectral method (Tamisiea et al., 2010) up to spherical harmonic degree 360 in the center of mass (CM) of the whole

Earth system frame. The load Love numbers used to determine the geoid and solid Earth response are computed from the Preliminary Referenced Earth Model (Dziewonski & Anderson (1981)). The resulting relative sea level change $\eta(\theta, \phi, t)$ at longitude θ, latitude ϕ, and time t can then be expressed as follows:

$$\eta(\theta, \phi, t) = G(\theta, \phi, t) - R(\theta, \phi, t) + \mathcal{L}(t) \quad (1)$$

$G(\theta, \phi, t)$ is the deformation of the geoid, $R(\theta, \phi, t)$ is the change of the solid Earth height, and $\mathcal{L}(t)$ is a global mean term, which is required to ensure mass conservation. Hence, regional variations in relative sea level are both caused by changes in the local geoid and solid Earth deformation. $R(\theta, \phi, t)$ and $G(\theta, \phi, t)$ evaluate to zero when integrated over the whole Earth. However, they do not necessarily evaluate to zero when integrated over the global ocean or over the altimetry domain (±66°S). Therefore, $\mathcal{L}(t)$ is generally not equal to the total barystatic change.

Local geocentric sea level change $\zeta(\theta, \phi, t)$ only differs from local relative sea level change by the local solid Earth height change. Therefore, geocentric sea level change can be expressed as follows:

$$\zeta(\theta, \phi, t) = \eta(\theta, \phi, t) + R(\theta, \phi, t) = \mathcal{L}(t) + G(\theta, \phi, t) \quad (2)$$

Since geoid variations have more power at longer wavelengths than solid Earth deformations, the spatial patterns of relative sea level changes (equation (1)) can substantially differ from those of geocentric changes (equation (2)).

We compute the sea level response to mass redistribution related to glaciers, the Greenland and Antarctic ice sheets, and LWS over the period 1993–2014. We use the mass redistribution data from Frederikse et al. (2017), which provides estimates of the temporal and spatial distribution of the mass changes from the aforementioned processes, which we review here briefly. Glacier mass loss is based on a surface mass balance model (Marzeion et al., 2015). The Greenland and Antarctic ice sheet contributions are based on an input-output approach, where the surface mass balance (SMB) contribution is based on RACMO2.3 (van den Broeke et al., 2016; van Wessem et al., 2016). The ice discharge is modeled as a constant acceleration departing from long-term equilibrium between SMB and discharge before 1993. The acceleration is 6.6 Gt/yr^2 for the Greenland ice sheet and 2.0 Gt/yr^2 for the Antarctic ice sheet. The total mass change is partitioned over each ice sheet by normalized GRACE mascon solutions (Watkins et al., 2015). For LWS, we include groundwater depletion, based on modeled estimates from Wada et al. (2012), and dam retention, based on the GRaND dam database (Lehner et al., 2011), with reservoir filling and seepage rates from Chao et al. (2008). For a more complete description of the data and the associated uncertainties, we refer to Frederikse et al. (2016, 2017).

The barystatic contribution associated with each process is depicted in Figure 1a. To assess the impact on regional estimates, we have separated the ocean in six regions, as depicted in Figure 1b, which also shows the domain covered by the TOPEX/Poseidon and Jason 1/2/3 altimeters, which is between ±66°S.

To estimate the impact of corrections for VLM on tide gauge-based reconstructions, we apply the virtual station method (Jevrejeva et al., 2006) on our synthetic sea level change field. First, we sample our synthetic sea level change field at the tide gauge locations from the revised local reference (RLR) database from the Permanent Service for Mean Sea Level (PSMSL; Holgate et al. (2013)). To avoid the inclusion of locations where the record is incomplete or where the tide gauge station has been abandoned, we only use station locations for which more than 15 valid annual sea level observations between 1993 and 2014 are available, which results in 627 station locations. Each station location is linked to an ocean basin, as depicted in Figure 1b. Second, the sampled sea level time series are merged into a basin mean reconstruction using the virtual station method, in which the two closest stations in each basin are combined into a new virtual station located halfway both stations, until only one station is left per basin. The final remaining virtual station that results from this interpolation is used as a proxy for the full basin. A global mean is computed by averaging the basin reconstructions, weighted by the individual basin sizes. Since our synthetic data field does not contain data gaps or has issues related to unknown reference levels, we compute a simple arithmetic mean between the time series of the two merged stations to compute a new virtual station.

3. The Spatial Pattern of the Relative and Geocentric Sea Level Response

The rates of elastic ocean bottom deformation (expressed in the center of mass (CM) frame), relative sea level, and geocentric sea level changes due to the aforementioned mass redistribution processes are shown in

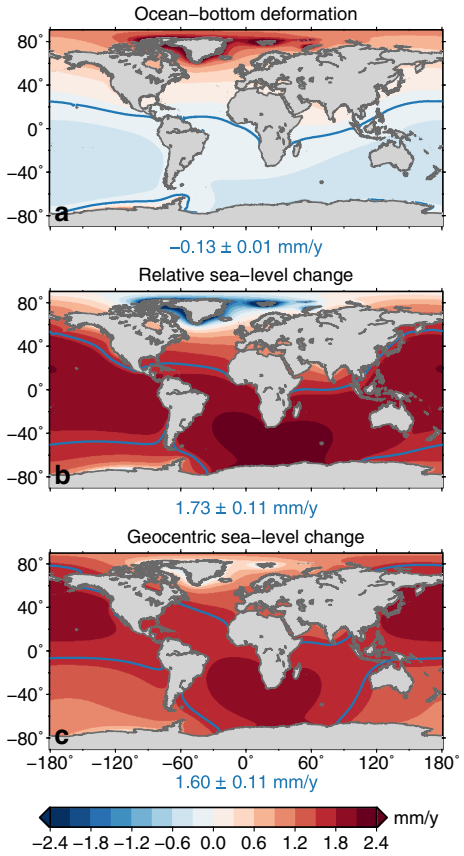

Figure 2. Linear trends and accompanying 1σ confidence intervals resulting from ice mass and LWS changes over 1993–2014 in (a) solid Earth deformation over the oceans, (b) relative sea level, and (c) geocentric sea level. Note that geocentric sea level change is equivalent to the sum of relative sea level and ocean bottom deformation change. The blue line depicts the line where local sea level change is equal to the ocean mean sea level trend, whose value is written in blue under each map.

Figure 2, together with the ocean mean rates. Due to the increase of the total ocean load, the ocean bottom on average elastically deforms by −0.13 mm/yr over 1993–2014 (Figure 2a). This subsidence is in addition to the routinely considered effects of GIA, which cause a global mean ocean bottom deformation of about −0.15 to −0.4 mm/yr (Tamisiea, 2011), as well as regional deformation patterns. Due to differences in the underlying physical processes, the elastic pattern considered here differs substantially from the GIA-related pattern (Mitrovica & Milne, 2002). As a result of the fact that the rate of global mean ocean bottom deformation is negative, the ocean bottom on average subsides, and the global mean rate of geocentric sea level change is smaller than the global mean relative sea level change (i.e., global ocean volume change).

The rate of elastic subsidence shows distinct spatial features: an uplift signal is present close to the major melt sources around the Arctic Ocean, Alaska, and the West Antarctic ice sheet. A north-south gradient is visible in Figure 2a, with large parts of the Northern Hemisphere oceans showing uplift, while most of the Southern Hemisphere is affected by a subsidence rate above the global mean. This ocean bottom deformation signal determines a large part of the regional variability of the resulting relative sea level changes depicted in Figure 2b, especially close to the major ice melt sources, while the variations in geocentric sea level changes, for which the regional variability is only determined by geoid changes, show smaller spatial gradients (Figure 2c). Therefore, the largest differences between relative and geocentric sea level can be found in high-latitude areas close to the major ice melt sources.

The observed north-south pattern in Figure 2a suggests that motion of the geocenter plays a role in the observed deformation. A substantial part of the surface mass redistribution is caused by mass loss from Greenland and the glacierized regions surrounding the Arctic Ocean. This surface mass is redistributed over

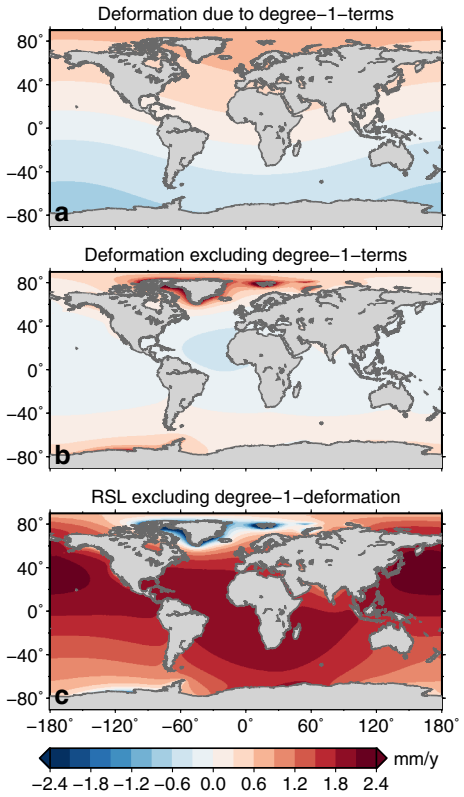

Figure 3. Ocean bottom deformation in the CM frame related to geocenter motion. (a) Ocean bottom deformation caused by the degree 1 terms. (b) Ocean bottom deformation from all other spherical harmonic terms. The sum of Figures 3a and 3b equals the ocean bottom deformation as shown in Figure 2a. (c) Relative sea level change excluding the degree 1 term in solid Earth deformation.

the oceans, resulting in a net southward shift of the Earth center of mass in the center of figure frame. As a result, in the center of mass (CM) frame, the solid Earth shifts northward, which causes uplift in the north and subsidence in the south. We explore this shift by examining the resulting deformation from the three degree 1 spherical harmonics of the solid Earth deformation field, which is depicted in Figure 3a.

The figure shows that the solid Earth deformation related to geocenter motion explains a substantial part of the spatial signal at low frequencies. Due to this large signal, the near-field uplift resulting from mass loss at the West Antarctic ice sheet is barely visible in Figure 2a. The removal of the geocenter-related signal (Figure 3b) reveals that the influence of Antarctic uplift reaches over large parts of the Southern Oceans. The signal related to geocenter motion also affects the relative sea level fingerprint, depicted in Figure 3c. Compared to Figure 2c, the impact of mass loss in West Antarctica becomes more visible. A substantial part of the uncertainties in reference frame realizations, which affect multiple geodetic observations, including satellite altimetry and GPS, is related to geocenter motion (Riddell et al., 2017; Santamaría-Gómez et al., 2017). Since geocenter motion-related effects form a substantial contribution to the spatial patterns of sea level changes and bottom deformation, the observed spatial patterns from satellite altimetry and VLM-corrected tide gauges will be affected by this uncertainty.

Because ocean bottom deformation has a distinct regional pattern, its effect will vary between individual ocean basins. The resulting time series per basin, together with the linear trends, are shown in Figure 4.

For most regions, the relative sea level trend exceeds the geocentric trend. The difference in the trend varies between 0.04 mm/yr in the North Pacific and 0.41 mm/yr in the South Pacific. However, for the North Atlantic and Arctic Oceans, both close to major sources of ice mass loss, the geocentric sea level trend exceeds the relative sea level trend. In the Arctic Ocean, the large regional uplift results in a negative rate of relative sea level rise, while geocentric sea level rise is still positive.

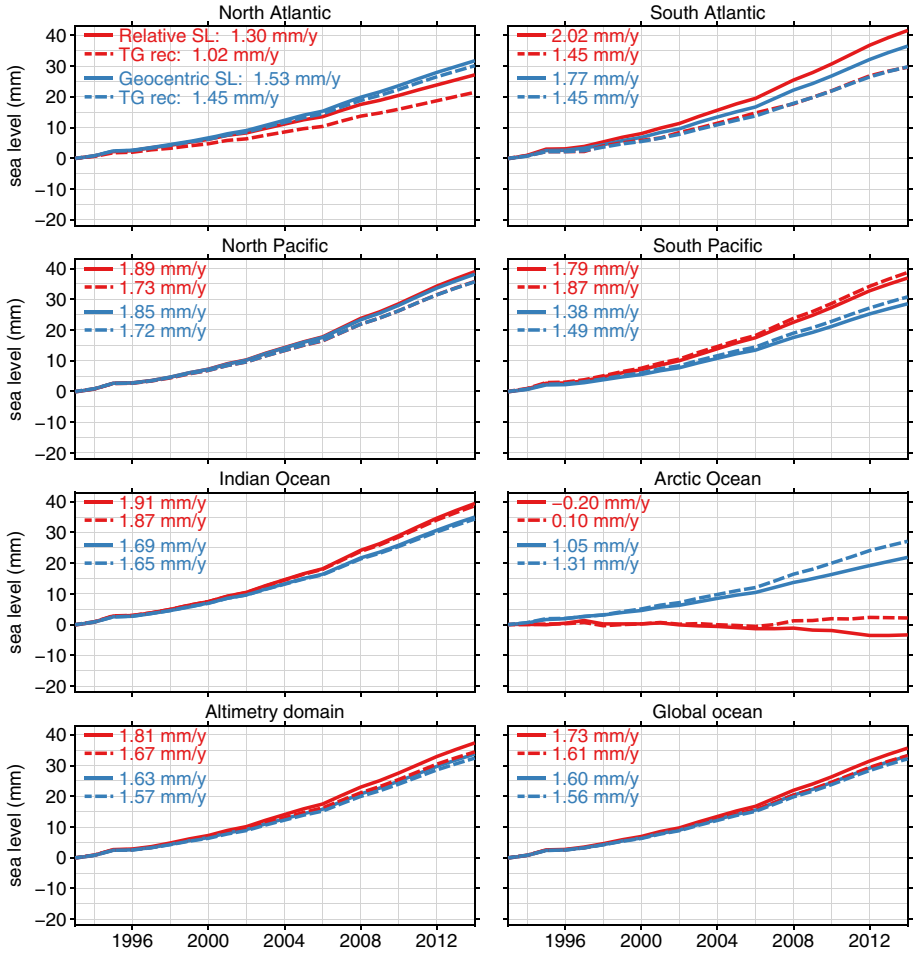

Figure 4. Basin-averaged and global mean effects of present-day mass redistribution on observed relative and geocentric sea level change. The solid line represents the average spatial signal over each region. The dashed line ("TG rec") represents tide gauge reconstructions based on the virtual station method using the locations of the 627 PSMSL tide gauges. The altimetry domain consists of the global oceans, bounded by ±66° latitude. For the virtual station estimate of the altimetry domain, all regions except the Arctic Ocean region are used.

4. The Effect on Tide Gauge Reconstructions

Since tide gauge observations only sample the ocean at a limited number of locations, the difference between relative and geocentric sea level changes reconstructed from tide gauge records may diverge from the underlying basin mean or global mean difference. In this section, we estimate the size of this difference due to present-day mass redistribution in VLM-corrected tide gauge reconstructions. We reconstruct basin mean and global sea level changes due to present-day mass loss using the virtual station method. The synthetic relative and geocentric sea level fields, as depicted in Figure 2, are sampled at 627 tide gauge locations, as described in section 2. We assume that the solid Earth deformation is observed at the same grid cell as the tide gauge location. In practice, the distance between the tide gauge and VLM observations often amounts to many kilometers, which may cause an additional bias, especially in areas where a large spatial gradient in the deformation field is present.

Results from the basin mean and global reconstruction are depicted as the dashed lines in Figure 4. At regional scales, reconstructions of basin mean relative and geocentric sea level show distinct differences, which are generally similar in sign and magnitude to the differences computed from averaging the deformation field over the whole basin, as discussed in the previous section, although the uneven sampling of the tide gauge records over the basins results in differences with the basin mean values, especially in the South Atlantic, where the relative and geocentric sea level reconstructions both deviate substantially from the original values.

Averaged over the global ocean, the difference between the synthetic geocentric and relative sea level reconstructions is only 0.05 mm/yr, which is smaller than the difference in the underlying basin mean trends, which is 0.13 mm/yr. This small difference suggests the effect of present-day surface mass redistribution is small on global reconstructions based on tide gauge records that have been corrected for observed VLM. The reconstructed difference becomes larger when the high-latitude tide gauges are omitted ("Altimetry domain") but is still smaller than the difference in the underlying fields. It should be noted that both the global relative and geocentric sea level changes are underestimated by the tide gauge reconstructions, as also found by Thompson et al. (2016), who note a 0.1 mm/yr underestimation when sea level is sampled at 15 tide gauges with long records, instead of the 627 tide gauge locations used in this study.

5. Discussion and Conclusions

We have quantified the effect of present-day mass loss on elastic ocean bottom deformation, which results in differences between global and basin mean relative and geocentric sea level changes. This difference affects a multitude of sea level observations. Over 1993–2014, global mean geocentric sea level has risen about 8% less than the barystatic equivalent. Hence, if globally covering satellite altimeters would observe sea level, due to present-day mass redistribution, the total volume increase would be underestimated by about 0.13 mm/yr. However, due to choices in the satellite orbits, the area covered by altimetry observations is generally limited, and the highest latitudes are often not observed. When GMSL is estimated from the range covered by the TOPEX/Poseidon and Jason altimeters, as depicted in Figure 1, the underestimation of the total volume change becomes about 0.10 mm/yr or 6% of the barystatic contribution. Note that next to barystatic sea level rise, steric changes are present, and hence, total GMSL rise over 1993–2014, which is in the order of 3 mm/yr (Chambers et al., 2016; Chen et al., 2017) and is larger than the barystatic contribution alone. Because the elastic response of the Earth is reasonably well defined (Mitrovica et al., 2011), the uncertainty of the correction is largely due to uncertainties in the mass redistribution.

The global mean ocean bottom deformation due to elastic deformation caused by present-day mass redistribution is still smaller than the ocean bottom deformation bias that results from the viscoelastic response to ice mass changes in the past (GIA), which is in the order of −0.15 to −0.4 mm/yr (Tamisiea, 2011). Furthermore, the bias is still within the uncertainty range of altimetry-derived GMSL trends, which are in the order of 0.4 mm/yr (Chen et al., 2017). Nevertheless, the effect is systematic and relatively easy to account for. In a future warming climate, the sea level rise induced by ice sheets will increase (e.g., Kopp et al., 2014), and therefore, the magnitude of the bias due to elastic ocean bottom deformation will grow. When we assume no changes in the altimetry trend uncertainty, the bias becomes larger than the uncertainty when barystatic sea level rise reaches 6.5 mm/yr. Under high-end sea level rise scenarios, such barystatic contributions could be reached during the 21st century (DeConto & Pollard, 2016; Jevrejeva et al., 2016).

Ocean bottom deformation varies spatially, and on regional and basin mean scales, the resulting difference between geocentric and relative sea level can deviate substantially. The largest differences can be found in the Arctic Ocean: due to the location close to many melt sources, the relative sea level in the Arctic drops, while geocentric sea level rises, resulting in a 1.3 mm/yr difference between both metrics. Outside the Arctic Ocean, basin mean differences up to 0.4 mm/yr or 23% of the regional relative sea level changes occur. Although the spatial patterns show substantially less variability compared to the patterns related to ocean dynamic changes, the differences between geocentric and relative sea level are in the same range as uncertainties in basin mean sea level estimates from altimetry, which are on the submillimeter level in many basins (Kleinherenbrink et al., 2016; Purkey et al., 2014).

In reconstructions in which no direct VLM observations or satellite altimetry are used (e.g., Hay et al., 2015; Jevrejeva et al., 2006), the effects of ocean bottom deformation will not affect the reconstructions, although the sampling of the spatially varying sea level field by the limited number of tide gauges may result in a bias (Thompson et al., 2016). Recently, VLM-corrected tide gauge observations have been used to reconstruct regional and global mean sea level changes (Dangendorf et al., 2017; Wöppelmann et al., 2014). Tide gauge reconstructions observe geocentric sea level changes when the records are corrected for VLM. Therefore, bottom deformation could affect these reconstructions as well. Using the virtual station technique using all locations of the PSMSL RLR database with 70% data availability over the altimetry area, we only find a small difference between reconstructed global mean geocentric and relative sea level. We do find that the reconstruction of global mean relative sea level underestimates the underlying basin mean value, which was also

noticed by Thompson et al. (2016). Leaving the Arctic Ocean out of the tide gauge reconstructions results in a larger difference between geocentric and relative sea level changes, although the aforementioned bias with the underlying basin mean sea level changes is still present. On regional scales, we find similar differences between relative and geocentric sea level changes for the synthetic tide gauge reconstruction as for the averaged fields, although in some basins, especially in the South Atlantic Ocean, the sparse sampling results in differences with the underlying fields. The differences between relative and geocentric sea level in global and regional tide gauge reconstructions are not independent from the station selection and reconstruction method, and the aforementioned values cannot be blindly used to quantify the effect of bottom deformation in a specific reconstruction. For example, the global reconstruction from Church and White (2011) uses spatial sea level change patterns estimated from altimetry, which are also affected by ocean bottom deformation, although in a different way than mentioned here.

Since the differences between relative and geocentric sea level change are caused by deformation of the solid Earth, they should be observable in VLM estimates at coastal locations. However, the uncertainties of individual VLM observations and 20 year linear trends in tide gauge observations are still generally larger than the rates considered here (Dangendorf et al., 2014; Hughes & Williams, 2010; Wöppelmann & Marcos, 2016). On regional scales, when multiple independent observations can be combined, analyses do suggest that ocean bottom deformation resulting from present-day mass loss can be observed in GPS and tide gauge records (Galassi & Spada, 2017; Pfeffer et al., 2017).

Since barystatic sea level rise shows an acceleration over the last two decades (Chen et al., 2017), altimetry and VLM-corrected tide gauge observations also underestimate the global mean sea level acceleration. The mass contribution to sea level rise is expected to increase further in a warming climate, and hence, this bias will also increase toward levels that possibly exceed the margins of uncertainty at individual tide gauge locations.

To increase the accuracy of sea level estimates, the effect of ocean bottom deformation should be taken into account, either based on modeled estimates of ocean mass change, as was done in this study, or using more direct observations. For example, the GRACE mission allows direct estimates of global mass redistribution, from which ocean bottom deformation can be computed (Ray et al., 2013), although with uncertainty associated with models of glacial isostatic adjustment (King et al., 2012). The large regional differences require caution when tide gauge and altimetry observations are compared on a regional scale or when regional volume changes are estimated from observations in a geocentric reference frame.

Acknowledgments

The authors would like to thank Ben Marzeion, Michiel van den Broeke, and Yoshihide Wada for sharing the models that have been used to estimate mass redistribution. All pictures have been produced using the Generic Mapping Tools. The deformation data are available from the corresponding author upon request. R. E. M. R. and T. F. acknowledge funding from The Netherlands Organisation for Scientific Research (NWO) through VIDI grant 864.12.012. M. A. K. is a recipient of an Australian Research Council Future Fellowship (project FT110100207) and supported by the Australian Research Council Special Research Initiative for Antarctic Gateway Partnership (Project ID SR140300001) and Discovery Project ID DP150100615. A data repository containing the time-varying solid Earth deformation fields and relative sea level changes can be found at http://doi.org/10.4121/uuid:1fb477a9-12ac-44a2-ae1d-d233b2673304.

References

Chambers, D. P., Cazenave, A., Champollion, N., Dieng, H., Llovel, W., Forsberg, R., … Wada, Y. (2016). Evaluation of the global mean sea level budget between 1993 and 2014. *Surveys in Geophysics*, *38*(1), 309–327. https://doi.org/10.1007/s10712-016-9381-3

Chao, B. F., Wu, Y. H., & Li, Y. S. (2008). Impact of artificial reservoir water impoundment on global sea level. *Science*, *320*(5873), 212–4. https://doi.org/10.1126/science.1154580

Chen, X., Zhang, X., Church, J. A., Watson, C. S., King, M. A., Monselesan, D., … Harig, C. (2017). The increasing rate of global mean sea-level rise during 1993–2014. *Nature Climate Change*, *7*(7), 492–495. https://doi.org/10.1038/nclimate3325

Church, J. A., & White, N. J. (2011). Sea-level rise from the late 19th to the early 21st century. *Surveys In Geophysics*, *32*(4–5), 585–602. https://doi.org/10.1007/s10712-011-9119-1

Clark, J. A., & Lingle, C. (1977). Future sea-level changes due to West Antarctic ice sheet fluctuations. *Nature*, *269*(5625), 206–209. https://doi.org/10.1038/269206a0

Dangendorf, S., Calafat, F. M., Arns, A., Wahl, T., Haigh, I. D., & Jensen, J. (2014). Mean sea level variability in the North Sea: Processes and implications. *Journal of Geophysical Research: Oceans*, *119*, 6820–6841. https://doi.org/10.1002/2014JC009901

Dangendorf, S., Marcos, M., Wöppelmann, G., Conrad, C. P., Frederikse, T., & Riva, R. (2017). Reassessment of 20th century global mean sea level rise. *Proceedings of the National Academy of Sciences*, *114*, 5946–5951. https://doi.org/10.1073/pnas.1616007114

DeConto, R. M., & Pollard, D. (2016). Contribution of Antarctica to past and future sea-level rise. *Nature*, *531*(7596), 591–597. https://doi.org/10.1038/nature17145

Dziewonski, A. M., & Anderson, D. L. (1981). Preliminary reference Earth model. *Physics of the Earth and Planetary Interiors*, *25*(4), 297–356. https://doi.org/10.1016/0031-9201(81)90046-7

Fenoglio-Marc, L., Rietbroek, R., Grayek, S., Becker, M., Kusche, J., & Stanev, E. (2012). Water mass variation in the Mediterranean and Black Seas. *Journal of Geodynamics*, *59*, 168–182. https://doi.org/10.1016/j.jog.2012.04.001

Frederikse, T., Riva, R., Kleinherenbrink, M., Wada, Y., van den Broeke, M., & Marzeion, B. (2016). Closing the sea level budget on a regional scale: Trends and variability on the Northwestern European continental shelf. *Geophysical Research Letters*, *43*, 10,864–10,872. https://doi.org/10.1002/2016GL070750

Frederikse, T., Simon, K., Katsman, C. A., & Riva, R. (2017). The sea-level budget along the Northwest Atlantic coast: GIA, mass changes and large-scale ocean dynamics. *Journal of Geophysical Research: Oceans*, *122*, 5486–5501. https://doi.org/10.1002/2017JC012699

Galassi, G., & Spada, G. (2017). Tide gauge observations in Antarctica (1958–2014) and recent ice loss. *Antarctic Science*, *29*(4), 369–381. https://doi.org/10.1017/S0954102016000729

Hay, C. C., Morrow, E., Kopp, R. E., & Mitrovica, J. X. (2015). Probabilistic reanalysis of twentieth-century sea-level rise. *Nature*, *517*(7535), 481–484. https://doi.org/10.1038/nature14093

Holgate, S. J., Matthews, A., Woodworth, P. L., Rickards, L. J., Tamisiea, M. E., Bradshaw, E., … Pugh, J. (2013). New data systems and products at the permanent service for mean sea level. *Journal of Coastal Research*, *29*, 493–504. https://doi.org/10.2112/JCOASTRES-D-12-00175.1

Hughes, C. W., & Williams, S. D. P. (2010). The color of sea level: Importance of spatial variations in spectral shape for assessing the significance of trends. *Journal Of Geophysical Research*, *115*, C10048. https://doi.org/10.1029/2010JC006102

Jevrejeva, S., Grinsted, A., Moore, J. C., & Holgate, S. (2006). Nonlinear trends and multiyear cycles in sea level records. *Journal Of Geophysical Research*, *111*, C09012. https://doi.org/10.1029/2005JC003229

Jevrejeva, S., Jackson, L. P., Riva, R. E. M., Grinsted, A., & Moore, J. C. (2016). Coastal sea level rise with warming above 2 °C. *Proceedings of the National Academy of Sciences*, *113*(47), 13,342–13,347. https://doi.org/10.1073/pnas.1605312113

King, M. A., Keshin, M., Whitehouse, P. L., Thomas, I. D., Milne, G., & Riva, R. E. M. (2012). Regional biases in absolute sea-level estimates from tide gauge data due to residual unmodeled vertical land movement. *Geophysical Research Letters*, *39*, L14604. https://doi.org/10.1029/2012GL052348

Kleinherenbrink, M., Riva, R., & Sun, Y. (2016). Sub-basin-scale sea level budgets from satellite altimetry, Argo floats and satellite gravimetry: A case study in the North Atlantic Ocean. *Ocean Science*, *12*(6), 1179–1203. https://doi.org/10.5194/os-12-1179-2016

Kopp, R. E., Horton, R. M., Little, C. M., Mitrovica, J. X., Oppenheimer, M., Rasmussen, D. J., … Tebaldi, C. (2014). Probabilistic 21st and 22nd century sea-level projections at a global network of tide-gauge sites. *Earth's Future*, *2*(8), 383–406. https://doi.org/10.1002/2014EF000239

Kuo, C.-Y., Shum, C. K., Guo, J.-y., Yi, Y., Braun, A., Fukumori, I., … Shibuya, K. (2008). Southern Ocean mass variation studies using GRACE and satellite altimetry. *Earth, Planets and Space*, *60*(5), 477–485. https://doi.org/10.1186/BF03352814

Lehner, B., Liermann, C. R., Revenga, C., Vörösmarty, C., Fekete, B., Crouzet, P., … Wisser, D. (2011). High-resolution mapping of the world's reservoirs and dams for sustainable river-flow management. *Frontiers in Ecology and the Environment*, *9*(9), 494–502. https://doi.org/10.1890/100125

Leuliette, E. W., & Willis, J. K. (2011). Balancing the sea level budget. *Oceanography*, *24*, 122–129. https://doi.org/10.5670/oceanog.2011.32

Marzeion, B., Leclercq, P. W., Cogley, J. G., & Jarosch, A. H. (2015). Brief communication: Global reconstructions of glacier mass change during the 20th century are consistent. *The Cryosphere*, *9*(6), 2399–2404. https://doi.org/10.5194/tc-9-2399-2015

Milne, G. A., & Mitrovica, J. X. (1998). Postglacial sea-level change on a rotating Earth. *Geophysical Journal International*, *133*(1), 1–19. https://doi.org/10.1046/j.1365-246X.1998.1331455.x

Mitrovica, J. X., & Milne, G. A. (2002). On the origin of late Holocene sea-level highstands within equatorial ocean basins. *Quaternary Science Reviews*, *21*(20), 2179–2190. https://doi.org/10.1016/S0277-3791(02)00080-X

Mitrovica, J. X., Gomez, N., Morrow, E., Hay, C., Latychev, K., & Tamisiea, M. E. (2011). On the robustness of predictions of sea level fingerprints. *Geophysical Journal International*, *187*(2), 729–742. https://doi.org/10.1111/j.1365-246X.2011.05090.x

Nerem, R. S., Chambers, D. P., Choe, C., & Mitchum, G. T. (2010). Estimating mean sea level change from the TOPEX and Jason altimeter missions. *Marine Geodesy*, *33*(S1), 435–446. https://doi.org/10.1080/01490419.2010.491031

Pfeffer, J., Spada, G., Mėmin, A., Boy, J. P., & Allemand, P. (2017). Decoding the origins of vertical land motions observed today at coasts. *Geophysical Journal International*, *210*(1), 148. https://doi.org/10.1093/gji/ggx142

Purkey, S. G., Johnson, G. C., & Chambers, D. P. (2014). Relative contributions of ocean mass and deep steric changes to sea level rise between 1993 and 2013. *Journal of Geophysical Research: Oceans*, *119*, 7509–7522. https://doi.org/10.1002/2014JC010180

Ray, R. D., Beckley, B. D., & Lemoine, F. G. (2010). Vertical crustal motion derived from satellite altimetry and tide gauges, and comparisons with DORIS measurements. *Advances in Space Research*, *45*(12), 1510–1522. https://doi.org/10.1016/j.asr.2010.02.020

Ray, R. D., Luthcke, S. B., & van Dam, T. (2013). Monthly crustal loading corrections for satellite altimetry. *Journal of Atmospheric and Oceanic Technology*, *30*(5), 999–1005. https://doi.org/10.1175/JTECH-D-12-00152.1

Riddell, A. R., King, M. A., Watson, C. S., Sun, Y., Riva, R. E., & Rietbroek, R. (2017). Uncertainty in geocenter estimates in the context of ITRF2014. *Journal of Geophysical Research: Solid Earth*, *122*, 4020–4032. https://doi.org/10.1002/2016JB013698

Rietbroek, R., Brunnabend, S.-E., Kusche, J., Schröter, J., & Dahle, C. (2016). Revisiting the contemporary sea-level budget on global and regional scales. *Proceedings of the National Academy of Sciences*, *113*(6), 1504–1509. https://doi.org/10.1073/pnas.1519132113

Riva, R. E. M., Frederikse, T., King, M. A., Marzeion, B., & van den Broeke, M. (2017). Brief communication: The global signature of post-1900 land ice wastage on vertical land motion. *The Cryosphere*, *11*(3), 1327–1332. https://doi.org/10.5194/tc-11-1327-2017

Santamaría-Gómez, A., Gravelle, M., Dangendorf, S., Marcos, M., Spada, G., & Wöppelmann, G. (2017). Uncertainty of the 20th century sea-level rise due to vertical land motion errors. *Earth and Planetary Science Letters*, *473*, 24–32. https://doi.org/10.1016/j.epsl.2017.05.038

Stammer, D., Cazenave, A., Ponte, R. M., & Tamisiea, M. E. (2013). Causes for contemporary regional sea level changes. *Annual Review of Marine Science*, *5*, 21–46. https://doi.org/10.1146/annurev-marine-121211-172406

Tamisiea, M. E. (2011). Ongoing glacial isostatic contributions to observations of sea level change. *Geophysical Journal International*, *186*(3), 1036–1044. https://doi.org/10.1111/j.1365-246X.2011.05116.x

Tamisiea, M. E., Hill, E. M., Ponte, R. M., Davis, J. L., Velicogna, I., & Vinogradova, N. T. (2010). Impact of self-attraction and loading on the annual cycle in sea level. *Journal of Geophysical Research*, *115*, C07004. https://doi.org/10.1029/2009JC005687

Thompson, P. R., Hamlington, B. D., Landerer, F. W., & Adhikari, S. (2016). Are long tide gauge records in the wrong place to measure global mean sea level rise? *Geophysical Research Letters*, *43*, 10,403–10,411. https://doi.org/10.1002/2016GL070552

van den Broeke, M. R., Enderlin, E. M., Howat, I. M., Kuipers Munneke, P., Noël, B. P. Y., van de Berg, W. J., … Wouters, B. (2016). *On the recent contribution of the Greenland ice sheet to sea level change, The Cryosphere*, *10*(5), 1933–1946. https://doi.org/10.5194/tc-10-1933-2016

van Wessem, J. M., Ligtenberg, S. R. M., Reijmer, C. H., van de Berg, W. J., van den Broeke, M. R., Barrand, N. E., … van Meijgaard, E. (2016). The modelled surface mass balance of the Antarctic Peninsula at 5.5 km horizontal resolution. *The Cryosphere*, *10*(1), 271–285. https://doi.org/10.5194/tc-10-271-2016

Wada, Y., van Beek, L. P. H., Sperna Weiland, F. C., Chao, B. F., Wu, Y.-H., & Bierkens, M. F. P. (2012). Past and future contribution of global groundwater depletion to sea-level rise. *Geophysical Research Letters*, *39*, L09402. https://doi.org/10.1029/2012GL051230

Watkins, M. M., Wiese, D. N., Yuan, D.-N., Boening, C., & Landerer, F. W. (2015). Improved methods for observing Earth's time variable mass distribution with GRACE using spherical cap mascons. *Journal of Geophysical Research: Solid Earth*, *120*, 2648–2671. https://doi.org/10.1002/2014JB011547

Wöppelmann, G., & Marcos, M. (2016). Vertical land motion as a key to understanding sea level change and variability. *Reviews of Geophysics*, *54*, 64–92. https://doi.org/10.1002/2015RG000502

Wöppelmann, G., Marcos, M., Santamaría-Gómez, A., Martín-Míguez, B., Bouin, M.-N., & Gravelle, M. (2014). Evidence for a differential sea level rise between hemispheres over the twentieth century. *Geophysical Research Letters*, *41*, 1639–1643. https://doi.org/10.1002/2013GL059039